Low-latitude ionospheric-thermospheric response to storm time electrodynamical coupling between high and low latitudes

Mala S. Bagiya,[1] K. N. Iyer,[1] H. P. Joshi,[1] Smitha V. Thampi,[2] Takuya Tsugawa,[3] Sudha Ravindran,[4] R. Sridharan,[4] and B. M. Pathan[5]

Received 18 June 2010; revised 2 October 2010; accepted 19 October 2010; published 13 January 2011.

[1] Using multi-instrumental and multistation data, we present low-latitude ionospheric-thermospheric behavior during the geomagnetic storm of 15 May 2005. The diurnal pattern of total electron content (TEC) at a chain of equatorial to low-latitude stations shows strong positive ionospheric storm on 15 May. Latitudinal variation of TEC shows development of strong equatorial ionization anomaly (EIA) on the same day. Evidence, in terms of equatorial electrojet (EEJ) and magnetogram signatures, is presented for the prompt penetration of interplanetary electric field (IEF) as the cause of the positive ionospheric storm. Consequent to the storm time circulation resulting from the extra energy deposition via Joule heating over high latitudes, compositional changes occur in the global thermosphere. TEC enhancements on 16 May are attributed to enhancement of atomic oxygen at equatorial and low latitudes and the negative ionospheric storm on 17 May observed beyond certain low latitudes is explained in terms of enhancement of molecular species because of the storm time neutral composition changes. Strong ESF plume structures on range time intensity (RTI) map and L-band scintillation and TEC depletions in GPS measurements are observed in the longitude sectors where the local time of sudden storm commencement (SSC) falls after the post sunset hours. The ionospheric zonal electric fields are altered by the combined effects of eastward disturbance dynamo electric fields and direct prompt penetration of eastward electric fields associated with the northward turning of interplanetary magnetic field (IMF) B_z leading to subsequent development of ESF after midnight.

Citation: Bagiya, M. S., K. N. Iyer, H. P. Joshi, S. V. Thampi, T. Tsugawa, S. Ravindran, R. Sridharan, and B. M. Pathan (2011), Low-latitude ionospheric-thermospheric response to storm time electrodynamical coupling between high and low latitudes, *J. Geophys. Res.*, *116*, A01303, doi:10.1029/2010JA015845.

1. Introduction

[2] During geomagnetically disturbed conditions, ionospheric electric fields and currents at equatorial and low latitudes have been observed to be modulated by the direct prompt penetration of a dawn-dusk electric field to equatorial and low-latitude ionosphere [*Nishida*, 1968; *Spiro et al.*, 1988; *Sastri et al.*, 1997] and by the ionospheric disturbance dynamo electric field [*Blanc and Richmond*, 1980; *Fejer and Scherliess*, 1997]. The storm time ionospheric electric field perturbations often affect the distribution of ionospheric plasma by creating positive ionospheric storm (increased electron density) and/or negative ionospheric storm (decreased electron density) and the occurrence of plasma density irregularities at equatorial and low latitudes [e.g., *Fejer*, 1986; *Abdu et al.*, 1991; *Abdu*, 1997; *Sobral et al.*, 1997; *Sastri et al.*, 2000; *Basu et al.*, 2001a].

[3] The southward turning of interplanetary magnetic field (IMF) B_z during geomagnetic storms makes possible the transfer of tremendous amount of solar wind energy and particles to the magnetosphere. The resulting convection electric fields and DP2 currents were observed to penetrate to the equatorial ionosphere during the substorm growth phase [*Kelley et al.*, 1979; *Fejer et al.*, 1979; *Gonzales et al.*, 1979; *Somayajulu et al.*, 1987; *Kikuchi et al.*, 2000a]. Quasi periodic DP2 magnetic fluctuations are caused by the convection electric fields controlled by the IMF [*Nishida*, 1968]. *Kikuchi et al.* [2008] have shown the penetration of intense convection electric field to the equator which drives the DP2 currents at the dayside geomagnetic equator with magnitude greater than the diurnal variation. The reversal of IMF B_z to northward during geomagnetic storm causes a depletion in convection electric field; because of this the electric fields at midlatitudes and low latitudes are observed

[1]Department of Physics, Saurashtra University, Rajkot, India.
[2]Research Institute for Sustainable Humanosphere, Kyoto University, Kyoto, Japan.
[3]National Institute of Information and Communications Technology, Tokyo, Japan.
[4]Space Physics Laboratory, Vikram Sarabhai Space Centre, Trivandrum, India.
[5]Indian Institute of Geomagnetism, Navi Mumbai, India.

0148-0227/11/2010JA015845

to become reversed [*Rastogi and Patel*, 1975; *Kelley et al.*, 1979; *Fejer et al.*, 1979; *Gonzales et al.*, 1979; *Kobea et al.*, 2000; *Kikuchi et al.*, 2000b, 2003].

[4] The prompt penetration of electric field generally occurs during the period of large and rapid changes in magnetospheric convection and at the time of preliminary geomagnetic sudden commencement and sudden changes in the dynamic solar wind pressure. The penetration electric field is generally composed of convection electric field and overshielding electric field [*Fejer et al.*, 1979] which are active during the main phase and recovery phase of the storm, respectively [*Kikuchi et al.*, 2008]. The plasma sheet plasma move earthward because of the enhanced convection field and drives a partial ring current. During this the shielding electric fields are built up toward the equator of the auroral latitudes [*Vasyliunas*, 1972; *Jaggi and Wolf*, 1973; *Southwood*, 1977; *Senior and Blanc*, 1984]. After the shielding electric field produces, the electric fields at midlatitudes and low latitudes are often reversed when the convection electric field is decreased suddenly because of the northward turning of the IMF B_z. [*Rastogi and Patel*, 1975; *Kelley et al.*, 1979; *Fejer et al.*, 1979; *Gonzales et al.*, 1979; *Kobea et al.*, 2000; *Kikuchi et al.*, 2000b, 2003]. This reversal of the penetrated electric field is known as the overshielding electric field [*Kelley et al.*, 1979; *Gonzales et al.*, 1979; *Fejer et al.*, 1979].

[5] The prompt penetration of electric field is eastward during the daytime to the dusk sector and westward in the midnight to dawn sector [*Jaggi and Wolf*, 1973; *Spiro et al.*, 1988; *Fejer et al.*, 1990]. Therefore, it enhances the daytime eastward dynamo electric field and vertical drifts at equatorial and low-latitude ionosphere which lifts the plasma to greater altitudes, where the ratio of production to loss is greater, leading to enhanced electron densities in the dayside sector. The dayside ionospheric response to the prompt penetration electric field is seen as huge enhancement in TEC [*Maruyama et al.*, 2004; *Tsurutani et al.*, 2004] and the night side response is often observed as depletion in TEC [*Abdu et al.*, 2007]. In addition to this, the equatorial ionization anomaly (EIA) is found to intensify in amplitude as well as in latitudinal extent in association with the prompt penetration electric field [*Lin et al.*, 2005; *Mannucci et al.*, 2005; *Zhao et al.*, 2005; *Balan et al.*, 2010].

[6] The disturbance dynamo electric fields resulting from the enhanced energy deposition into the high latitude ionosphere are more slowly varying and perturb the low-latitude ionosphere during and up to about a day or two after the onset of geomagnetic storm, i.e., long-lived electrodynamical disturbances. [*Blanc and Richmond*, 1980; *Fejer et al.*, 1983; *Sastri*, 1988; *Mazaudier and Venkateswaran*, 1990; *Fejer*, 1997]. Disturbance dynamo electric field is westward in dayside, i.e., opposite to the daytime ionospheric dynamo electric field and eastward in the nightside. It can cause depletion of TEC in dayside [*Tsurutani et al.*, 2004] (negative ionospheric storm) and also cause suppression of EIA, while on nightside, results are reported showing huge *F* layer uplift at nighttime and even resurgence of strong EIA [*Fuller-Rowell et al.*, 2002]. However, *Huang et al.* [2005] have argued that because of the high conductivity of the E region the DD electric field during daytime is rather weak.

[7] Since the ionosphere and thermosphere behave as a coupled system, the storm time electrodynamical perturbations in ionosphere get reflected in the thermospheric dynamics also and this makes the situation bit complex. Direct particle precipitation in the polar region increases the auroral electrojet (AE) current which results in the generation of atmospheric gravity waves (AGWs) owing to the joule heating by the AE current system. These waves which are known as traveling atmospheric disturbances (TADs) [*Hines*, 1960, 1974; *Richmond*, 1978; *Jing and Hunsucker*, 1993; *Balthazor and Moffett*, 1997] propagate toward the equator and redistribute the energy and momentum through viscous interactions, heat conduction, and frictional loss because of ion drag with a time delay of 24 h or more [*Prolss*, 1997; *Fuller-Rowell et al.*, 2002]. The enhanced joule heating over polar latitudes lifts the neutrals and drives them toward the low and equatorial latitudes, thereby changing thermospheric composition globally. The atomic species (e.g., O) being lighter lifts up first and reach to lower latitudes earlier, contributing in positive ionospheric storm [e.g., *Burns et al.*, 1995; *Field et al.*, 1998] while molecular species, e.g., N_2, O_2, etc., being heavier reach later and can cause negative ionospheric storm. The meridional wind circulation changes both in magnitude and direction following a storm. In general, meridional winds flow from the equator to polar region during daytime and the reverse happen during nighttime. During geomagnetic storm these patterns change drastically and wind flows from the poles to the equatorial region [*Liu and Edwards*, 1988].

[8] In the dusk sector, the zonal electric field perturbations at the equator during geomagnetic storms lead to development/inhibition of Equatorial spread *F* (ESF) irregularities which is determined by the local time dependence of the polarity and amplitude of electric field perturbations of the prompt penetration and disturbance dynamo type. It was believed initially that the percentage occurrence of ESF is reduced during geomagnetic storms [*Lyon et al.*, 1960]. With the advancement of time, it was found that geomagnetic storm affects the post midnight and post sunset ESF differently [*Chandra and Rastogi*, 1972a, 1972b; *Rastogi et al.*, 1978; *Rastogi and Woodman*, 1978; *Chandra and Vyas*, 1978]. It was revealed later that the post midnight ESF is triggered by the geomagnetic storm events [e.g., *Aarons et al.*, 1980]. The occurrences of post sunset ESF events are triggered by storm events on some days particularly during non-ESF season [e.g., *Aarons et al.*, 1980; *Rastogi et al.*, 1981]. *Abdu* [1997] suggested that the triggering or inhibition of ESF depends on the phase of the storm. The geomagnetic storm can initiate ESF in the post midnight sector because of abnormal upward reversals in the vertical plasma drift under the action of eastward electric fields of ionospheric disturbance dynamo (IDD) [*Kelley and Maruyama*, 1992; *Hysell and Burcham*, 1998] and also often because of penetration of eastward electric fields associated with northward turning of IMF Bz [*Kelley et al.*, 1979]. There are ample of studies reported which explain the development/inhibition of ESF during geomagnetic storm and the role of storm time perturbation electric fields during last three decades [*Aarons*, 1991; *Sastri et al.*, 1993; *Abdu et al.*, 1995; *Fejer et al.*, 1999; *Basu et al.*, 2001b, 2005;

Table 1. Details of GPS Stations

Name of Station	Geographic Latitude	Geographic Longitude	Geomagnetic Latitude
Rajkot (RAJ)	22.29°N	70.7°E	14.29°N
Trivandrum(TVM)	8.55°N	76.9°E	0.29°N
Bangalore (BNG)	12.58°N	77.4°E	4.32°N
Hyderabad (HYD)	17.48°N	78.4°E	9.22°N
Bhopal (BHP)	23.17°N	77.2°E	14.21°N
Delhi (DEL)	28.58°N	77.2°E	20.32°N
Arequipa Laser Station (AREQ)	−16.47° N	288.5°E	−6.48°N
Galapagos Permanent Station (GLPS)	−0.74°N	269.7°E	8.75°N
Taal Volcano Station (TVST)	14.03°N	121°E	4.3°N

Sobral et al., 2001; *Huang et al.*, 2005, *Huang and Chen*, 2008; *Tulasi Ram et al.*, 2008].

[9] In this paper, we report the response of the equatorial and low-latitude ionosphere-thermosphere system to 15 May 2005 geomagnetic storm using ionospheric data from different longitude sectors Storm time equatorial and low-altitude ionospheric characteristics like positive and negative ionospheric storms and its influence on development of EIA in the day side sector are shown. The role of electrodynamical and neutral dynamical coupling between high and low latitudes in terms of prompt penetration electric field, disturbance dynamo electric field and storm time thermospheric neutral composition changes in the observed TEC behavior are discussed. In the longitude sector where the prompt penetration occurred after the local dusk period, the presence of ESF irregularities and L-band scintillation is found to occur. The role of eastward disturbance dynamo electric field and direct prompt penetration of eastward electric field associated with the northward tuning IMF Bz is discussed in this regard.

2. Data Set and Method of Analysis

[10] GPS – TEC measurements from low-latitude station Rajkot located near the EIA crest, and the GPS – TEC measurements from a chain of ISRO GAGAN (GPS Aided Geo Augmented Navigation) GPS receivers along the 77–78°E longitude extending from magnetic equator to the EIA crest and beyond, also in the Indian region, and from Arequipa Laser Station (AREQ), Galapagos Permanent Station (GLPS), Taal Volcano Station (TVST) have been used to study the effects of geomagnetic storm at day and night sectors. The details of all these stations are given in Table 1. Jicamarca (−11.57°N, 283.8°E, −1.61°N) radar and ionosonde data (http://jro.igp.gob.pe/madrigal) have also been used to see the behavior of nighttime ionospheric *F* region during the storm.

[11] For Indian GPS stations, the slant TEC data have been recorded at a sampling rate of 60 s and then converted in to the VTEC according to the method described by *Bagiya et al.* [2009]. The mean of VTEC data from all the visible satellites with elevation mask of 30° has been derived at every 15 min for a given Ionospheric Pierce Point (IPP) and presented as a single TEC value for that IPP. Diurnal profiles for that IPP are then derived from the above VTEC values with a temporal resolution of 15 min. The temporal resolution for AREQ, GLPS and TVST GPS data is 30 s. The VTEC values are plotted for these stations along with the standard deviation of rate of TEC change index (ROTI) with 5 min temporal resolution to show the presence of scintillation if any.

[12] Symmetric ring current index SYM-H values are used to represent the evolution of the storm. The dawn to dusk component of the interplanetary electric field (IEF), i.e., IEFy, for the SSC day has been calculated using the interplanetary magnetic field B_z component and the solar wind velocity V_x. The B_z and V_x values are obtained from Advanced Composition Explorer (ACE) satellite (located at L1 point). The IEFy can be expressed as

$$IEF_y = V_x \times B_z \quad (1)$$

To translate the electric field values to the Earth's ionosphere, appropriate time delay is incorporated by the method described in detail by *Chakrabarty et al.* [2005]. The time delay comprises of three components. The travel time of the solar wind from the spacecraft to the subsolar bow shock (t_1), propagation time from the bow shock to the magnetopause (t_2), and the Alfven transit time (t_3) along the magnetic field lines from the subsolar magnetopause to the ionosphere. The estimated values for t_1 vary from ~59 min to ~24 min on 15 May, the estimated values for t_2 vary from ~0.097 min to 0.023 min. The average values for t_3 is taken as 2 min [*Khan and Cowley*, 1999]. The total time delay during the present storm is found to be varying from 61 min to 25 min.

[13] The absolute values of the horizontal magnetic field H component from four magnetic observatories extending from equator to midlatitudes around the longitude belt of 77 ±

Table 2. Details of Magnetometer Stations

Name of Station	Geographic Latitude	Geographic Longitude	Geomagnetic Latitude
Tirunelveli	8.7°N	77.8°E	0.32°N
Alibag	18.46°N	72.87°E	10.19°N
Alma Ata	43.25°N	76.92°E	34.29°N
Novosibirsk	55.03°N	82.9°E	45.57°N

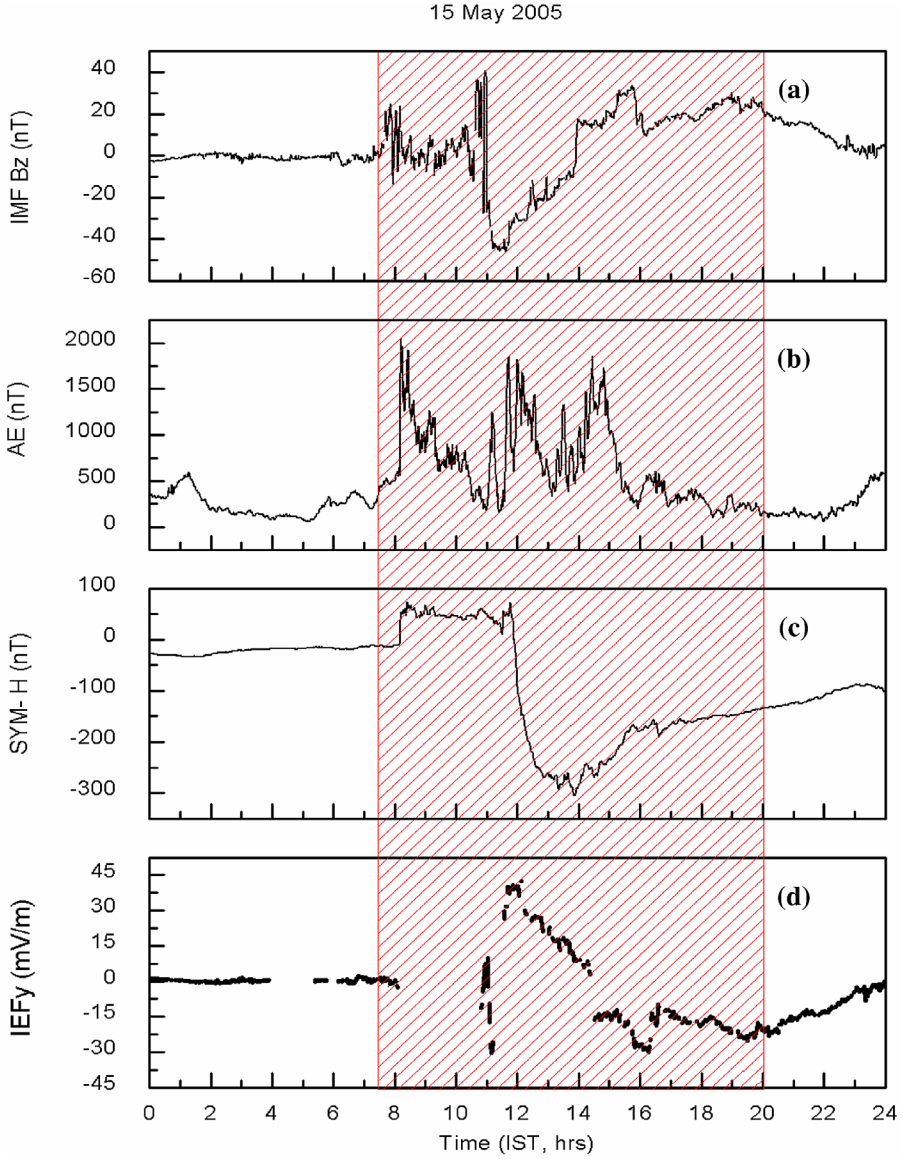

Figure 1. (a) Interplanetary magnetic field (IMF) B_z variations, (b) auroral electrojet (AE) index variations, (c) symmetric ring current index SYM-H, and (d) interplanetary electric field (IEF) y variations with time lag correction on 15 May 2005.

5°E have been replotted at a resolution of 1 min for the SSC day. The details of these observatories are given in Table 2. The EEJ strength ($\Delta H_{(TIRUNELVELI)} - \Delta H_{(ALIBAG)}$) has been derived from the ΔH values at Alibag (low latitude) and Tirunelveli (magnetic equator) during the storm period as per the method adopted by *Rastogi and Klobuchar* [1990].

[14] To examine the thermospheric neutral composition changes during the storm period $[O]/[N_2]$ ratios have been extracted from TIMED/GUVI measurements and replotted for Indian latitude-longitude (lat-long) sectors. In the imaging mode the GUVI instrument of the TIMED satellite gives far ultraviolet images of thermosphere composition and temperature below about 625 km altitude. The details of the GUVI instrument, operation and example of data products are presented by *Paxton et al.* [1999, 2004] and *Christensen et al.* [2003]. The atomic oxygen to molecular nitrogen vertical column density ratio ($\Sigma O/N_2$) is one of the geophysical parameter obtained from data products of the GUVI imager. The ratio of vertical column density of atomic oxygen (135.6 nm) to that of molecular nitrogen (174.3 nm) is proportional to ratio of emission rates within the airglow layer, extending from about 140 km to 250 km [*Meier et al.*, 2005]. As the GUVI observations are not continuous for particular lat-long sector, the exact timing information for these observations is difficult to provide. But we have tried to derive the average time period of the GUVI $[O]/[N_2]$ observations and that falls in between 1150 IST to 1450 IST for Indian lat-long sectors for the presented days (IST = Indian Standard Time; IST = UT + 5.50 h).

3. Results and Discussion

[15] The geomagnetic storm of 15 May 2005 is unique in itself as the IEFy on occasion boosted to abnormally high

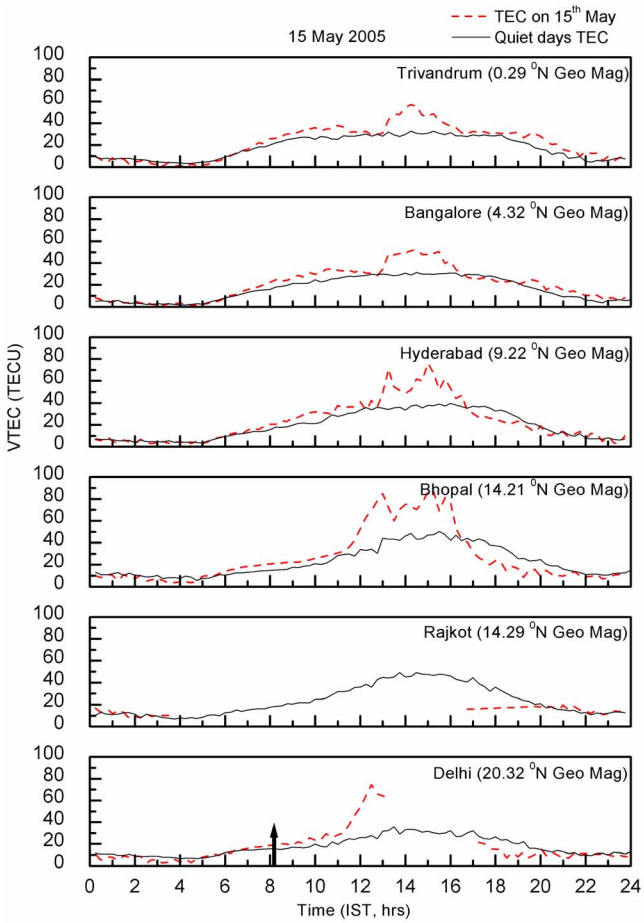

Figure 2a. Diurnal variation of total electron content (TEC) over stations located from equator to low latitude and beyond it on 15 May 2005.

values. Figures 1a, 1b, 1c and 1d show the temporal variations of appropriately time shifted IMF Bz, AE index, Sym-H index, and appropriately time shifted dawn to dusk component of IEFy, respectively, on 15 May 2005. The shaded area in Figure 1 shows the disturbed period on the day. The storm started with SSC at 0802 IST (0230 UT) just after the forward shock with amplitude of 39 nT synchronized with sudden increase in AE index on 15 May 2005. During the initial phase of the storm the SYM-H values remained steady at the raised value up to 1153 IST, after this SYM-H started to decrease very fast indicating the commencement of the main phase, and reaching a minimum value of −305 nT at 1351 IST. The main phase onset coincided in time with the southward turning of IMF Bz (negative), large AE index and a large IEFy values of ~42 mV/m. The data are not available for Vx for the time when sudden increase in AE index occurred (0804 IST to 1045 IST), therefore the initial variation of IEFy when SSC occurred cannot be presented.

3.1. Positive Ionospheric Storm on 15–16 May 2005

[16] Figure 2a illustrates TEC variations over the latitude belt (0.29°N to 20.30°N, geomagnetic) starting from Trivandrum (trough) to Bhopal (crest) and Delhi (beyond the crest of the EIA) on 15 May 2005 along with the quiet days' (Ap < 4) TEC mean of the month. An enhancement in TEC appeared first at low-latitude station Delhi and then at lower-latitude stations. The maximum amplitude of TEC enhancement of ~40 TECU with respect to quiet day's TEC appeared at EIA crest region Bhopal. Unfortunately, the data for Rajkot station is not available on this day, so could not be presented. The observed TEC enhancements from the equator to the low latitudes show strong positive ionospheric storm on 15 May. *Pandey and Dashora* [2006] have also observed daytime peak TEC of 100 TECU on 15 May 2005 from Udaipur (26.4°N 73.7°E, Geographic, 15.6°N Geomagnetic), India, another EIA crest station. *Mannucci et al.* [2005] reported the penetration of IEFy to the low and equatorial ionosphere causing ionospheric positive storm during the super storm of 29–30 October 2003. *Kelley et al.* [2003] invoked the penetration of strong high latitude electric field to the midlatitudes and low latitudes to explain the resultant daytime midlatitude TEC enhancements (Figure 2b).

[17] EEJ strength ($\Delta H_{(TIRUNELVELI)} - \Delta H_{(ALIBAG)}$) along with the magnetograms recorded on 15 May 2005 at stations spreading from equator to midlatitudes are plotted in Figure 3. Accompanying the IEFy increase (Figure 1d), EEJ increase started at 1100 IST, reached its maximum at 1120 IST, and started to decrease gradually at 1125 IST. The evolution of EEJ strength indicates that, EEJ maximum of ~220 nT occurred after the epoch when the IEFy increase is started. The absolute horizontal magnetic field values for Tirunelveli (Figure 3) also show sharp and significant increase which also almost coincides in time with maximum IEFy values at ~1145 IST. The observed EEJ strength of ~220 nT and simultaneous sharp increase in horizontal magnetic field values at Tirunelveli on 15 May provide evidence for the daytime prompt penetration of IEFy at low and equatorial latitudes. The penetrated electric field raises the *F* layer upward over the entire latitude belt, ranging from low latitudes to equator. At higher altitudes, the recombination rate will be slow resulting in resultant higher electron density at *F* layer altitudes.

[18] The midlatitude magnetograms (Alma Ata and Novosibirsk in Figure 3) are not showing any significant IEFy signatures. It is known that the midlatitude conductivity is low in comparison to the high and equatorial latitudes. *Reddy et al.* [1978] have stated that the high latitude electric field perturbations penetrate to the equatorial latitudes with reduction factors of ~10 in the longitude sector of the source region. Consequently, smaller electric field perturbations do not produce any significant surface magnetic field variations at midlatitudes. In the present case we can see that the IEFy values boosted to very high amplitude, but still we are not seeing any signatures of it at midlatitudes. The significant depression of H is progressively reduced with increasing distance from the equatorial station. The afternoon CEJ is seen shortly after the EEJ peak value of ~220 nT which coincides with the main phase of the storm. The northward turning of IMF Bz results in to the reversal of the electric fields at midlatitudes and low latitudes [*Rastogi and Patel*, 1975; *Kelley et al.*, 1979; *Fejer et al.*, 1979; *Gonzales et al.*, 1979; *Kobea et al.*, 2000; *Kikuchi et al.*, 2000b, 2003]. The reversal of penetrated electric fields results in the CEJ at the equator [*Rastogi and Patel*, 1975;

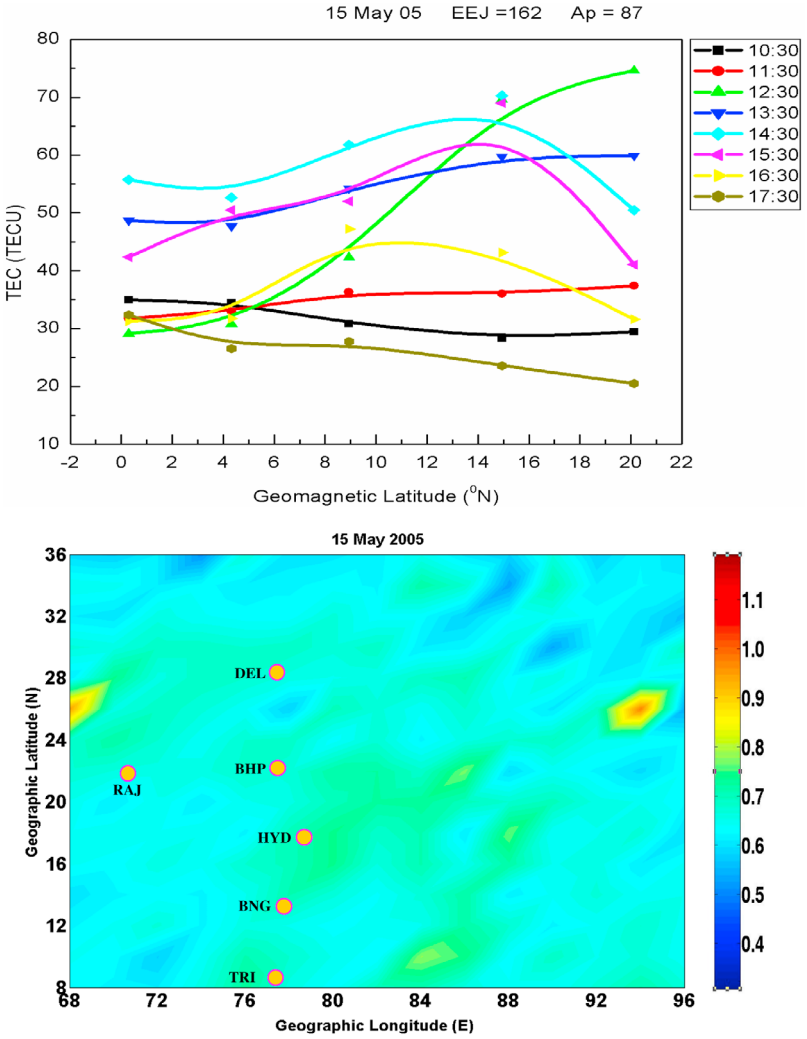

Figure 2b. (top) Latitudinal profiles of TEC starting from equatorial station Trivandrum (0.5°N, geomagnetic) to low-latitude station Delhi (20.38°N, geomagnetic) on 15 May 2005 at different day hours (time is in IST). (bottom) [O]/[N_2] values between 1150 Indian Standard Time (IST) to 1450 IST replotted for Indian latitude-longitude (lat-long) sector on 15 May 2005 derived from the observations of GUVI onboard the TIMED NASA satellite.

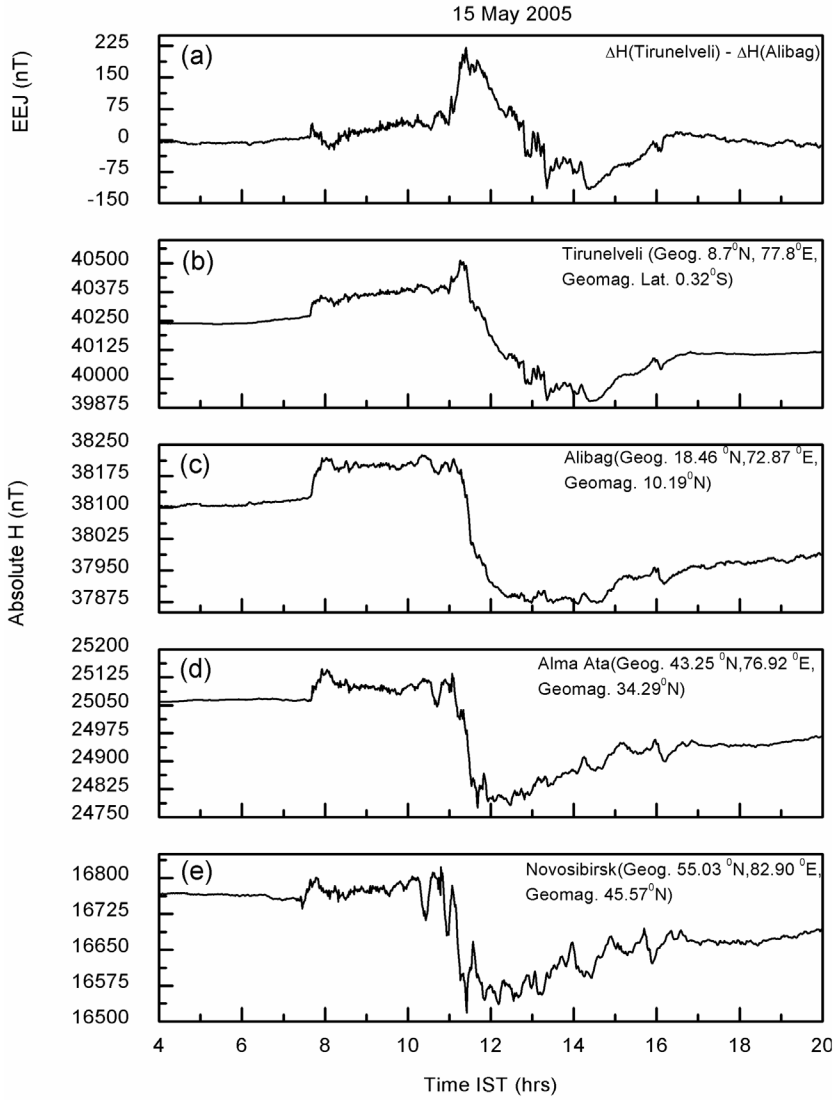

Figure 3. (a) Equatorial electrojet (EEJ) variation on 15 May 2005, (b) absolute values of H at equatorial station Tirunelveli, (c) absolute values of H at low-latitude station Alibag (18.6°N, 72.9°N, 12.9°N dip latitude) for the same day, (d) absolute values of H at midlatitude station Alma Ata, and (e) absolute values of H at another midlatitude station Novosibirsk on 15 May 2005.

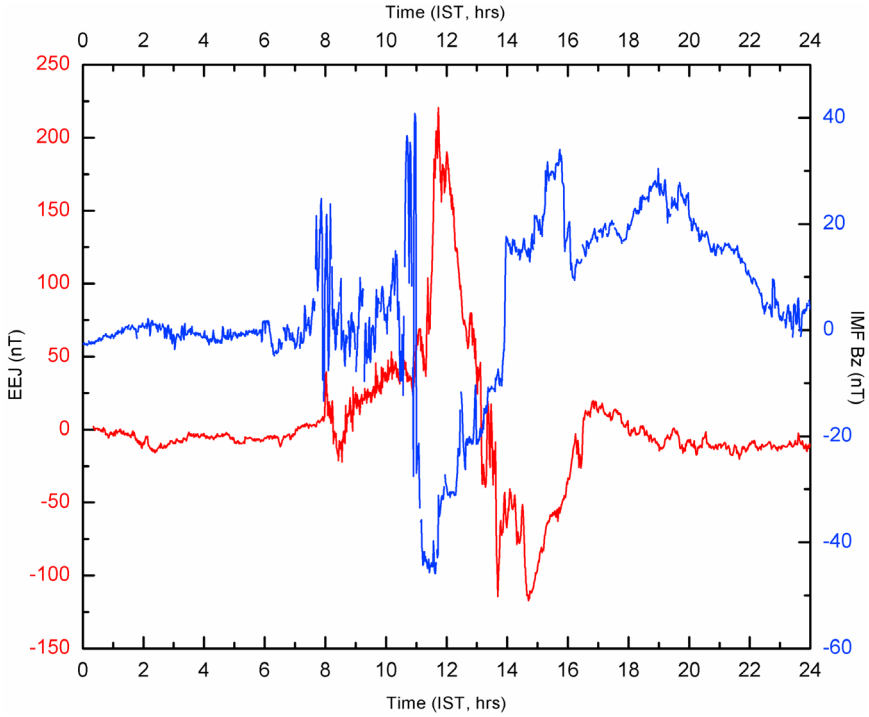

Figure 4. Diurnal variation of appropriately time shifted IMF B_z and EEJ on 15 May 2005.

Rastogi, 1977, 1997; *Kobea et al.*, 1998, 2000; *Kikuchi et al.*, 2000b, 2003, 2008]. Figure 4 shows the diurnal variation plot of IMF Bz and EEJ on 15 May 2005. It can be seen that CEJ initiation time coincides with the abrupt transition time of IMF Bz to northward. The convection electric field decreases rapidly with northward turning of IMF Bz and the resultant is the reversal of low-latitude electric fields.

[19] As seen in Figure 2a, depletion in TEC appeared at ~1300 IST at Trivandrum and Bangalore, simultaneous TEC enhancements developed at Hyderabad, Bhopal and Delhi. After 1300 IST, TEC increases at Trivandrum and Bangalore and simultaneous depletion is observed at Hyderabad, Bhopal and Delhi. The observed decrease in TEC at crest regions with simultaneous increase at trough regions on 15 May 2005 may be the effect of CEJ observed in the afternoon on 15 May 2005. The westward electric field during CEJ reverses **E** × **B** drifts thus plasma will start to return at trough latitudes because of reverse fountain effect. CEJ started to recover after 1400 IST. The second and gradual TEC increase at Hyderabad and Bhopal shortly after the depletion at ~1300 IST (Figure 2a) may be due to recovery of CEJ to the normal condition. The prompt variations of low-latitude TEC with respect to CEJ show the strong electrodynamical coupling between equatorial and low latitudes. The observed TEC enhancements at equatorial latitudes is followed by gradual decrease after 1600 IST while at crest latitudes the observed TEC depletion is followed by sharp increase between 1500 and 1600 IST. After 1600 IST, TEC shows regular daytime decrease at near crest and crest latitudes also.

[20] Figure 2b shows the development of EIA on 15 May 2005. EIA gets started to develop after 1030 IST. The

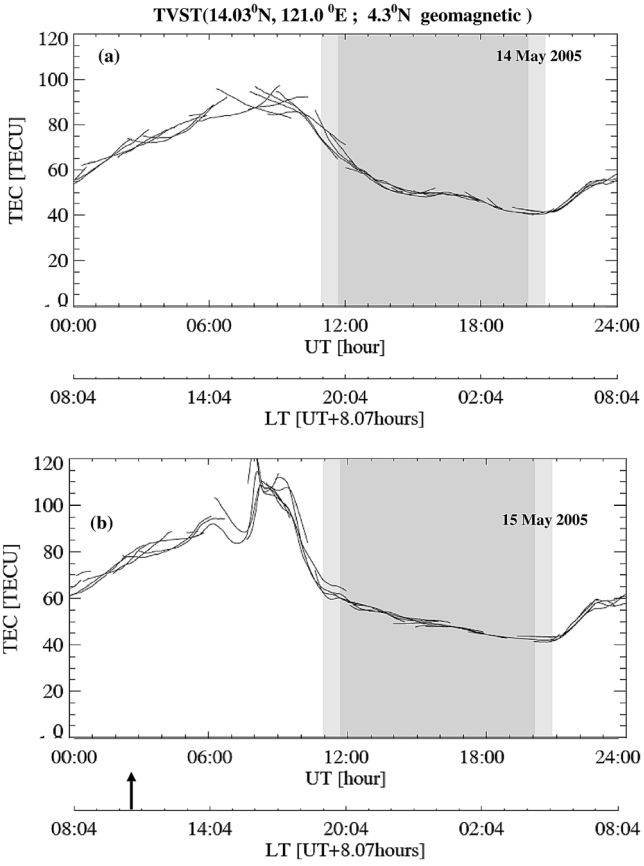

Figure 5. Diurnal VTEC variations at Taal Volcano Station (TVST) on (a) 14 May 2005 and (b) 15 May 2005.

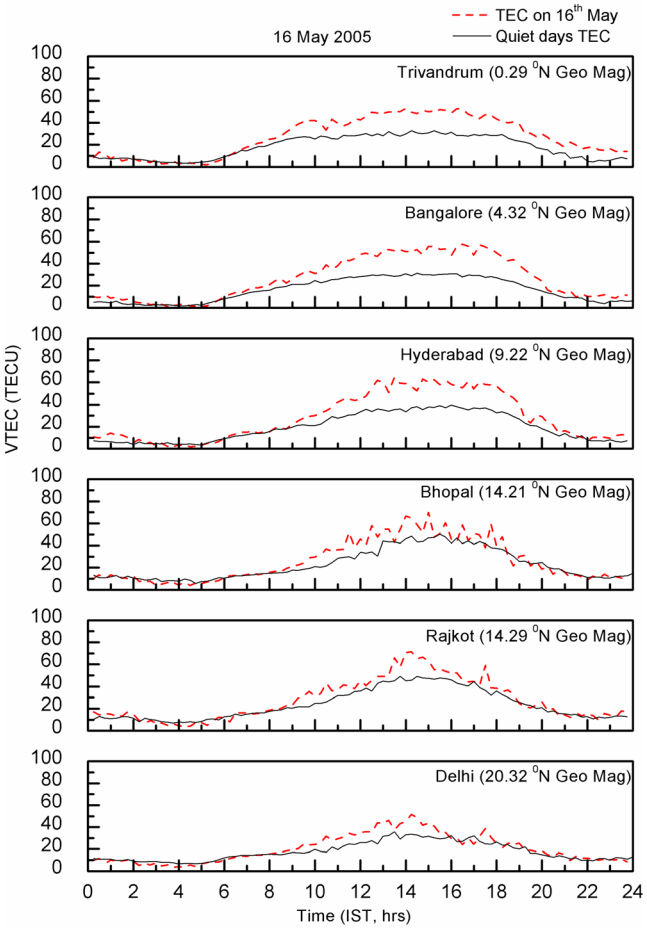

Figure 6a. Same as Figure 2a but for 16 May 2005.

strongest of EIA occurred at ~1230 IST shortly after the maximum of EEJ and extended up to ~21°N (geomagnetic) latitudes. The presence of intense EEJ on 15 May 2005 is an indication of high vertical E × B drift over the equator required for the strong EIA. As a result, TEC at the EIA crest, i.e., Bhopal and beyond crest, i.e., Delhi shows significance increase with respect to quiet days' mean, with maximum amplitude at Bhopal on the day. The strongest of EIA of the day at ~1230 IST is depressed by 1330 IST. The depressed EIA again redeveloped at ~1430 IST and then finally gets weakened gradually by ~1630 IST. The depression of EIA at 1330 IST also agrees with the reversal of zonal electric field at the equator. Because of the presence of afternoon CEJ, EIA strength reduces therefore electron density at trough latitudes increases and that at crest latitudes decreases. The TEC values are higher at ~1330, ~1430 and ~1530 IST than the values at 1230 IST at trough latitudes and are lower at crest latitudes. This indicates that intensity of EIA is decreasing after 1230 IST because of CEJ.

[21] The enhanced Joule heating in the polar region results in the development of equatorward neutral wind. These neutral winds carry molecular rich air toward mid and low latitudes, O being lighter arrives first. Hence initially an increase in $[O]/[N_2]$ is expected. The storm time thermospheric variations in terms of $[O]/[N_2]$ on 15 May 2005 is shown in Figure 2b (bottom). There is a significant increase in $[O]/[N_2]$ over the complete latitude belt of 8°N to 36°N around 77–78°E longitudes. As O is the major species which builds the *F* layer ionization, the increased value of $[O]/[N_2]$ contributes positively into the observed TEC enhancements.

[22] In addition to Indian longitude sector, data from other longitude sector where SSC occurred in daytime were also examined. Figures 5a and 5b represent the VTEC diurnal profiles for TVST on 14 and 15 May, respectively. Light and dark gray shadows represent nighttime at ionospheric heights. At TVST, the time of SSC is ~1030 LT (local time), indicated by arrow in Figure 5b. VTEC profile on 15 May 2005 shows that TEC has been increasing gradually after the SSC and the day maximum occurred delayed at ~1600 LT. The maximum TEC values observed are ~120 TECU at ~1600 LT which is higher by ~20 TECU than the TEC values observed on 14 May 2005. The gradual increase in TEC after the SSC is followed by a depletion of ~11 TECU at 1530 LT. This depletion is coincided with the minimum of main phase at TVST. This depletion is followed by sharp peak at ~1600 LT. The northward turning of IMF Bz results in to the CEJ which pulls the plasma from the crest latitudes toward the equatorial latitudes during fountain effect. Similar results have been observed for Indian region also.

[23] Figure 6a shows the diurnal TEC profiles on 16 May 2005 along with quiet days' (Ap < 4) mean TEC of the month for Rajkot and GAGAN stations, Figure 6b (top) represents the latitudinal TEC profiles for different hours on the day and Figure 6b (bottom) represents the $[O]/[N_2]$ variations for the Indian lat-long sectors on the day. On 16 May 2005, the day after the SSC event, significant daytime TEC enhancements are seen over the magnetic belt (0.29°N to 20.30°N, geomagnetic) starting from Trivandrum to Delhi with increase of ~20 TECU at Bhopal and ~12 TECU at Rajkot. But on 16 May 2005, increase over trough latitudes is clearer than the crest latitudes. The observed EIA profile on 16 May 2005, Figure 6b, shows that the EIA developed less pronouncedly with delayed peak at ~1330 IST. The neutral composition variations in Figure 6b (bottom) on 16 May shows considerable increase of $[O]/[N_2]$ at trough latitudes around 77–78°E longitudes and the increase is more clearer at trough latitudes. TEC enhancements have also been seen more effective at trough latitudes than the crest latitudes on 16 May 2005. This indicates that TEC enhancements on 16 May are caused by enhancement of O because of storm time neutral composition changes. From moderate EEJ values on 16 May 2005, it appears that there might be penetration of storm time disturbance dynamo electric field which gets activated ~4 h after the SSC phase and lasts up to about a day or two after the onset of geomagnetic storm [*Fejer et al.*, 2002, and reference therein]. The moderate EIA in Figure 6b agrees with the observed EEJ variations.

3.2. Negative Ionospheric Storm on 17 May 2005

[24] Figures 7a, 7b and 7c show ionospheric-themospheric behavior on 17 May 2005. It can be seen that clear increase in TEC on 16 May 2005 is followed by TEC depletion on 17 May 2005 at Rajkot of ~10 TECU and at Delhi of ~20 TECU. The observed TEC depletions represent the negative

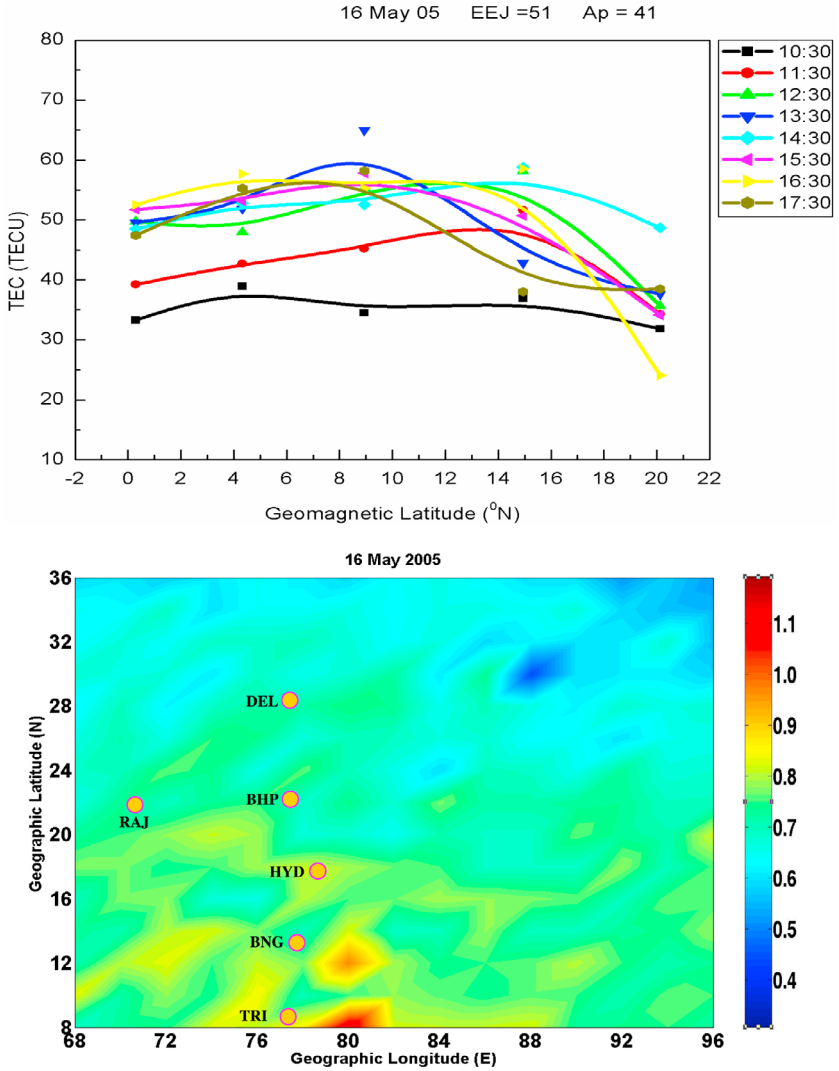

Figure 6b. (top) Same as Figure 2b (top) but for 16 May 2005. (bottom) Same as Figure 2b (bottom) but for 16 May 2005.

ionospheric storm and it appeared over low latitudes only and not observed below it.

[25] The value of $[O]/[N_2]$ was ~0.68 on 15 May 2005 over Rajkot region (Figure 2b, bottom). But on 17 May it decreased to 0.54 from 0.68 (Figure 7b, bottom). The $[O]/[N_2]$ depletion extended up to low-latitude region of ~16°N (magnetic) from the pole along the longitude belt of 77–78° indicating an enhancement of N_2. Electron loss at F_2 peak depends upon the recombination/attachment with N_2; as N_2 density increases, electron density decreases. Thus the observed negative storm on 17 May is due to storm time enhancement of molecular species. On 17 May 2005 EIA did not develop because of negative storm effect as seen in Figure 7b. Thus it can be said that neutral dynamical coupling dominant the electrodynamical coupling on 17 May 2005.

3.3. Local Time Dependent Response of ESF/ Scintillations

[26] A study has been carried out on the effects of geomagnetic storm over the equatorial and low-latitude ionosphere where local time of SSC falls after post sunset hours on 15 May 2005. At Jicamarca the local time of SSC is ~2130 LT, i.e., during premidnight hours. Figures 8a and 8b show JULIA (Jicamarca Unattended Long-Term Investigations of the Ionosphere and Atmosphere) RTI map on 13–14 May 2005 (a day before the onset of geomagnetic storm) and on 14–15 May 2005, respectively. The range time intensity (RTI) map gives information about the strength of the irregularities. On 13–14 May, the control day; ESF irregularities started to appear from ~1930 LT in valley-type format between 200 and 300 km with small updrafting patch at ~2200 LT. The ionosonde observations from Jicamarca

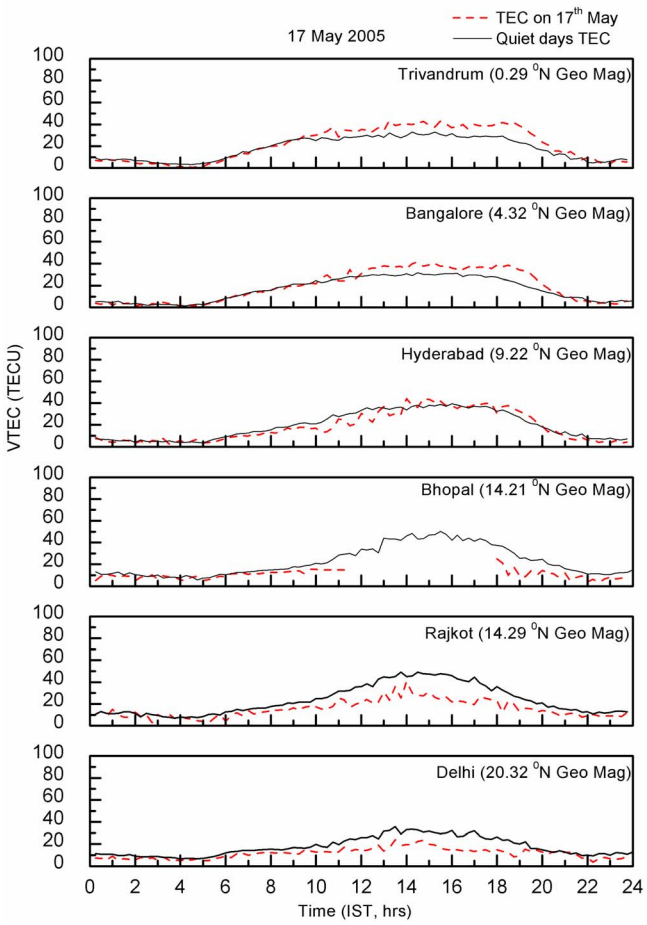

Figure 7a. Same as Figure 2a but for 17 May 2005.

(Figure 9a) on 13–14 May 2005 shows pre reversed rise in h′F after 1800 LT. Between 1800 LT and 1905 LT, an increase of ~50 km is seen in h′F. This prereversal enhancement creates necessary condition for the generation of ESF. GPS observations from AREQ in Figure 10a are not showing any significant scintillation on 13–14 May 2005. But at GLPS in Figure 11a TEC depletion in multiple PRNs (Pseudo Random Number, which is the identity number given to the different GPS satellites) associated with the high values of ROTI index is observed on 13–14 May 2005.

[27] On 14–15 May 2005 (SSC at ~2130 LT), Jicamarca ionosonde observations show gradual rise in h′F after local sunset but significant clear increase is seen at ~2130 LT which coincides with the onset of geomagnetic storm (Figure 9b). In radar backscattered map in Figure 8b, it can be seen that after 2130 LT, irregularities started to become strong and rising plume structure is seen between 2200 and 2300 LT with altitude range of 300 to 450 km. This coincides with the SSC. The rising plume started to descend after 2245 LT and again a strong band structure is seen up to 0045 LT. This band structure is ended with huge rising plume at ~0100 LT which coincides with the main phase of the storm. This second plume drifted up to more than 1000 km vertically.

[28] At AREQ the local time of SSC is ~2145 LT and at GLPS is ~2030 LT. When we look into the GPS observations at AREQ and GLPS on 14–15 May 2005, it can be seen that AREQ GPS observations show significant scintillation and TEC depletion between 2315 LT and 0215 LT (Figure 10b) which coincides with the main phase of the storm and second rising plumes of RTI map. At GLPS, TEC depletion and associated scintillation in ROTI values are seen after 2130 LT, i.e., 1 h after the local SSC time, on 14–15 May 2005 (Figure 11b). On 15 May 2005 the scintillation is absent up to 2000 LT at GLPS, after 2000 LT scintillation is started to develop and significant signatures are seen in ROTI index which are associated with the TEC depletion. This significant scintillation and associated TEC depletion coincided with the main phase of the storm as well as with the second rising plume at Jicamarca.

[29] The prompt penetration of electric field is eastward during the daytime to the dusk sector and westward in the midnight to dawn sector [*Jaggi and Wolf*, 1973; *Spiro et al.*, 1988; *Fejer et al.*, 1990]. In addition to this, the prompt penetration of eastward electric field at the dusk sector may add to the normal prereversal enhancement of zonal electric field because of the *F* region dynamo. The augmented vertical drift at the terminator creates more favorable conditions for the generation of Rayleigh-Taylor instability [*Ossakow*, 1981; *Sultan*, 1996] which leads to the development of ESF. *Kelley and Maruyama* [1992] and *Hysell and Burcham* [1998] have reported that the post midnight ESF can be triggered because of the eastward ionospheric disturbance dynamo electric field during geomagnetic storms. *Kelley et al.* [1979] have shown that the penetration of eastward electric fields associated with the northward turning of IMF Bz during geomagnetic storms can also often initiate the post midnight ESF. There are ample of results reported by *Rastogi and Woodman* [1978], *Aarons et al.* [1980], *Dabas et al.* [1989] and *Bowman* [1982] which show that the post midnight ESF tends to be triggered by geomagnetic storms.

[30] In the present case, the SSC has occurred at 0230 UT, the southward IMF Bz reverses its direction to northward ~0600 UT, i.e., almost after three and half hours of SSC. The strong ESF generation after midnight at Jicamarca is also after ~three and half hours of local time of SSC at Jicamarca. The depletion in convection field associated with the northward turning of IMF Bz makes weaken the westward ionospheric field. In addition to this the delayed effect in terms of disturbance dynamo electric field also modulates the ionospheric electric field depending on its polarity. The combined effect of both these leads to the generation of strong ESF irregularities after midnight.

[31] The significant h′F rise at 2130 LT and simultaneous generation of ESF plume as shown in RTI map at Jicamarca instantaneously at SSC time indicates that the prompt penetration of eastward electric field immediately after SSC provides platform for ESF generation on 14–15 May at Jicamarca. The second huge plume at 0045 LT, significant L-band scintillation at AREQ and GLPS around midnight provides evidence for the penetration of intense eastward electric fields associated with the northward turning of IMF Bz over the equator which prevailed over the ambient

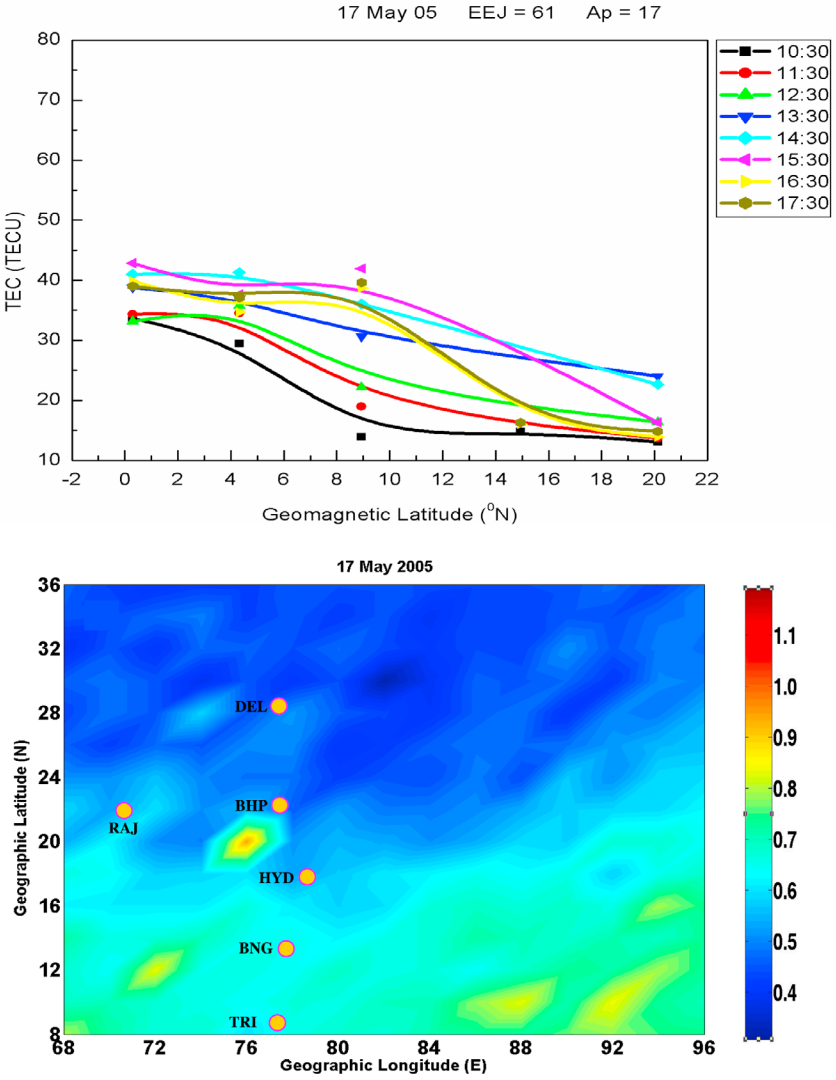

Figure 7b. (top) Same as Figure 2b (top) but for 17 May 2005. (bottom) Same as Figure 2b (bottom) but for 17 May 2005.

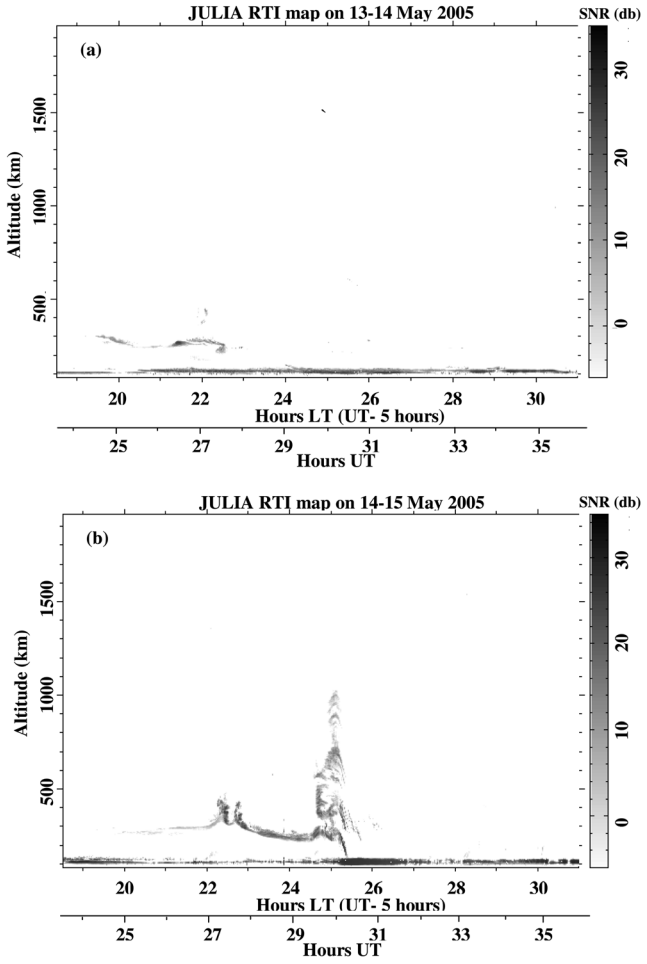

Figure 8. (a) Jicamarca Unattended Long-Term Investigations of the Ionosphere and Atmosphere (JULIA) range time intensity (RTI) map on 13–14 May 2005 and (b) JULIA RTI map on 14–15 May 2005.

westward electric fields leading to development of strong ESF after midnight. This corroborates with the previous report by *Tulasi Ram et al.* [2008]. Using the data from different longitude sectors, they explained the role of storm time prompt penetration of electric field in the occurrence of ESF.

4. Summary

[32] A detailed investigation is carried out on storm time electrodynamical and neutral dynamical coupling and its influences on the equatorial and low-latitude ionosphere for 15 May 2005 storm. The results and discussions presented in section 3 have shown that the storm time ionospheric perturbations because of either prompt penetration electric field or storm time neutral composition changes/disturbance dynamo electric field leads to positive and negative ionospheric storms, respectively. The storm time neutral composition variations on the day after the SSC day result in to the noticeable positive ionospheric storm on 16 May 2005. The combined effects of the penetration of eastward electric field associated with the northward turning of IMF Bz and eastward disturbance dynamo leads to the development of strong ESF plume after midnight.

[33] The main characteristics of this event can be highlighted as (1) the prompt penetration of electric field from high to low latitudes on 15 May 2005 as evident by intensified EEJ and sharp rise in absolute horizontal magnetic field values for Tirunelveli, results in to strong positive ionospheric storm in different longitude sectors during daytime. The prompt response of the equatorial and low-latitude TEC to CEJ variations on 15 May 2005 between 1300 IST and 1600 IST show strong electrodynamical coupling between low and equatorial latitudes. The sharp and correlated fluctuations in AE index, H values, EEJ strength and TEC are clear evidence of high-and low-latitude electrodynamical coupling during the storm. (2) On 16 May 2005, storm time neutral composition variations result in to higher $[O]/[N_2]$ values along 77–78°E longitudes with clearer

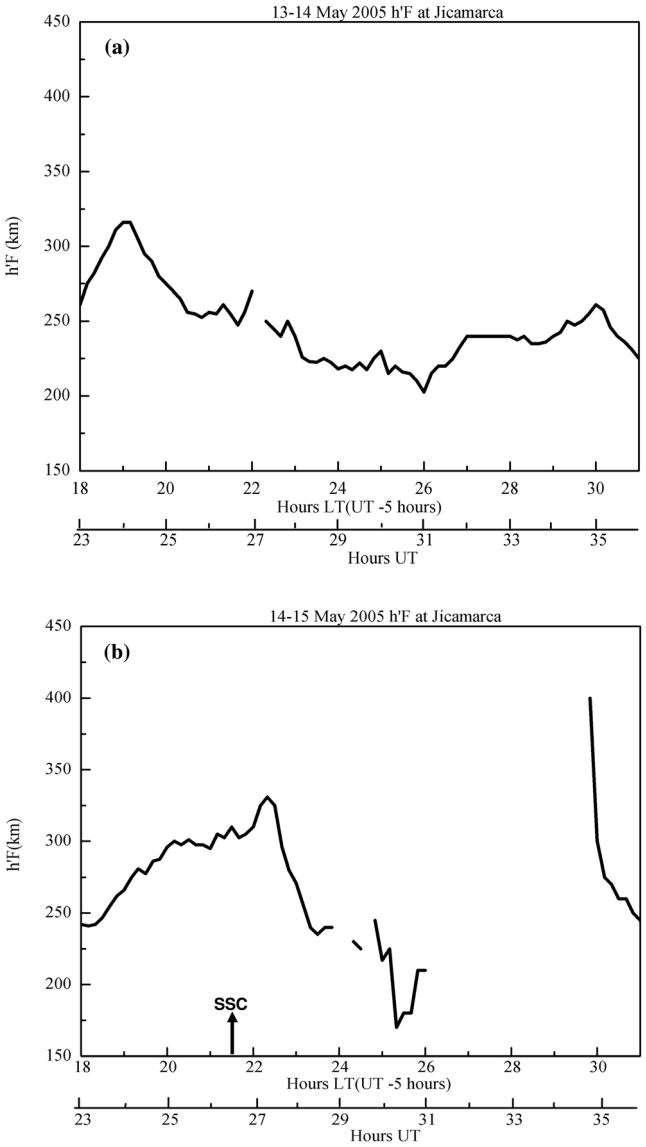

Figure 9. (a) The h′F variations at Jicamarca on 13–14 May 2005 and (b) h′F variations at Jicamarca on 14–15 May 2005.

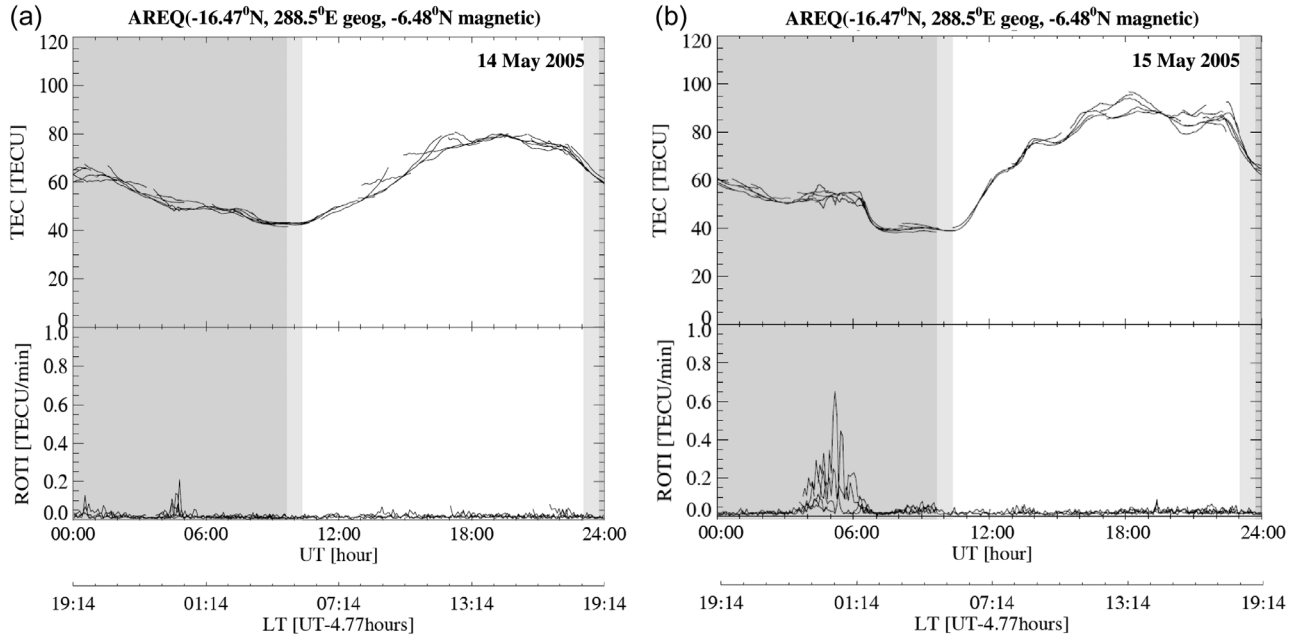

Figure 10. (a) Diurnal VTEC and ROTI variations at AREQ on 14 May 2005 and (b) diurnal VTEC and ROTI variations at AREQ on 15 May 2005.

increase at trough latitudes than at crest latitudes. A clear positive ionospheric storm is observed on 16 May 2005 also with more clear TEC enhancements at trough latitudes. (3) Low-latitude TEC shows negative storm effect on 17 May 2005. Delayed effects as on 16 and 17 May 2005 are evidences of thermosphere/neutral dynamical coupling. It is emphasized by the observations that positive effect of neutral composition variations is seen more clear at equatorial latitudes, i.e., atomics species can be enhanced up to equatorial latitudes while negative phase is seen only at Delhi and Rajkot (low latitudes) and not at equatorial latitudes, indicating that the effects of molecular enhancements do not penetrate beyond some limiting latitudes. (4) Vertically rising strong plume at Jicamarca after midnight as observed on RTI map and L-band scintillation and associated TEC depletion at AREQ and GLPS provide evidence for the

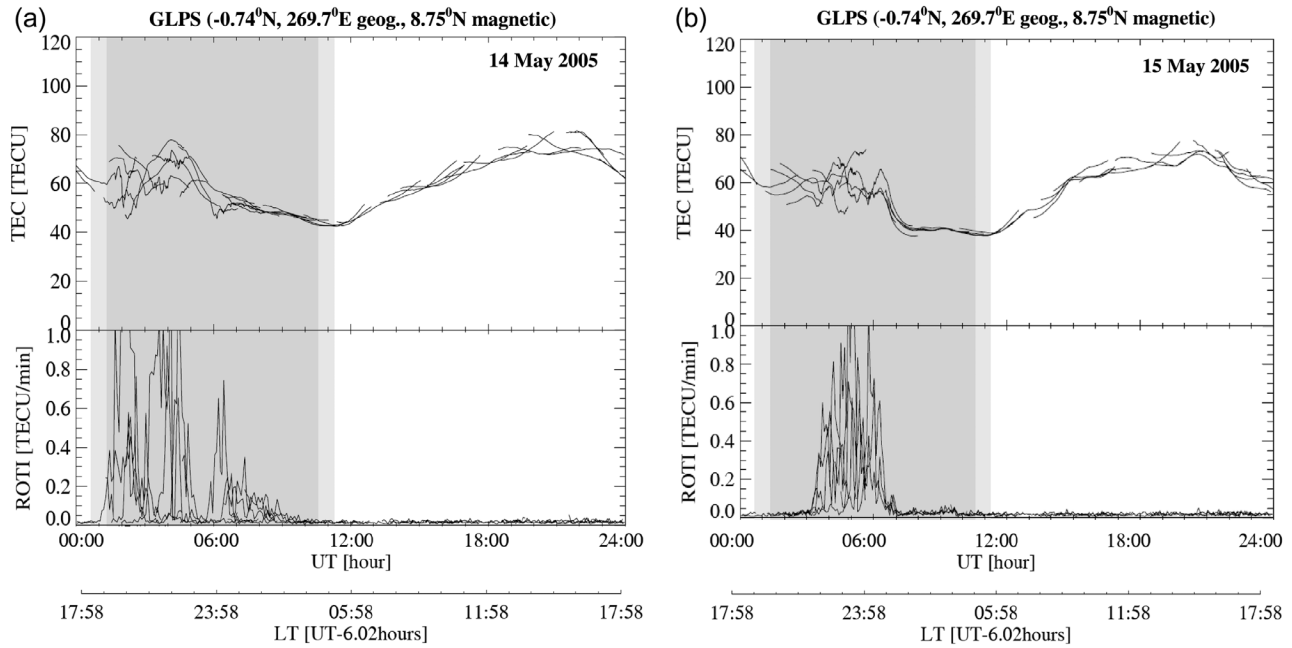

Figure 11. (a) Diurnal VTEC and rate of TEC change index (ROTI) variations at Galapagos Permanent Station (GLPS) on 14 May 2005 and (b) diurnal VTEC and ROTI variations at GLPS on 15 May 2005.

prompt penetration of eastward electric field associated with the northward turning of IMF Bz over the equator which prevailed over the strong westward electric fields in addition to the eastward disturbance dynamo electric field in midnight sector leading to the development of strong ESF plumes and significant L-band scintillation after midnight. The multi-instrumental and multistation data presented in this paper shows all the effects of geomagnetic storms over equatorial and low-latitude ionosphere-thermosphere system, and it is also seen that the prompt penetration of eastward electric fields into low latitudes and subsequent development of ESF occurred.

[34] **Acknowledgments.** We are thankful to Jicamarca Radio Observatory for providing us JULIA radar and ionosonde data. We thank NASA Data Center for providing us TIMED/GUVI images. We are thankful to World Data Center for Geomagnetism, Kyoto for providing us SYM-H, AE index values. We thank ACE SWEPAM and MAG teams as well as ACE science center for providing us the ACE data.

[35] Robert Lysak thanks the reviewers for their assistance in evaluating this paper.

References

Aarons, J. (1991), The role of ring current in the generation or inhibition of equatorial *F* layer irregularities during magnetic storms, *Radio Sci.*, *26*, 1131–1149, doi:10.1029/91RS00473.

Aarons, J., et al. (1980), Seasonal and geomagnetic control of equatorial scintillation in two longitudinal sectors, *J. Atmos. Terr. Phys.*, *42*, 861–866, doi:10.1016/0021-9169(80)90090-2.

Abdu, M. A. (1997), Major phenomena of the equatorial ionosphere-thermosphere system under disturbed conditions, *J. Atmos. Sol. Terr. Phys.*, *59*, 1505–1519.

Abdu, M. A., J. H. A. Sobral, E. R. de Paula, and I. S. Batisha (1991), Magnetospheric disturbance effects on the Equatorial Ionization Anomaly (EIA): An overview, *J. Atmos. Terr. Phys.*, *53*, 757–771, doi:10.1016/0021-9169(91)90126-R.

Abdu, M. A., I. S. Batista, G. O. Walker, J. H. A. Sobral, N. B. Trivedi, and E. R. de Paula (1995), Equatorial ionospheric fields during magnetospheric disturbances: Local time/longitudinal dependences from recent EITS Campaigns, *J. Atmos. Sol. Terr. Phys.*, *57*, 1065–1083, doi:10.1016/0021-9169(94)00123-6.

Abdu, M. A., T. Maruyama, I. S. Batista, S. Saito, and M. Nakamura (2007), Ionospheric responses to the October 2003 superstorm: Longitude/local time effects over equatorial low and middle latitudes, *J. Geophys. Res.*, *112*, A10306, doi:10.1029/2006JA012228.

Bagiya, M. S., H. P. Joshi, K. N. Iyer, M. Aggarwal, S. Ravindran, and B. M. Pathan (2009), TEC variations during low solar activity period (2005–2007) near the Equatorial Ionospheric Anomaly Crest region in India, *Ann. Geophys.*, *27*, 1047–1057, doi:10.5194/angeo-27-1047-2009.

Balan, N., K. Shiokawa, Y. Otsuka, T. Kikuchi, D. Vijaya Lekshmi, S. Kawamura, M. Yamamoto, and G. J. Bailey (2010), A physical mechanism of positive ionospheric storms at low latitudes and midlatitudes, *J. Geophys. Res.*, *115*, A02304, doi:10.1029/2009JA014515.

Balthazor, R. L., and R. J. Moffett (1997), A study of atmospheric gravity waves and travelling ionospheric disturbances at equatorial latitudes, *Ann. Geophys.*, *15*, 1048–1056, doi:10.1007/s00585-997-1048-4.

Basu, S., S. Basu, K. M. Groves, H.-C. Yeh, S.-Y. Su, F. J. Rich, P. J. Sultan, and M. J. Keskinen (2001a), Response of the equatorial ionosphere in the South Atlantic region to the great magnetic storm of July 15, 2000, *Geophys. Res. Lett.*, *28*, 3577–3580, doi:10.1029/2001GL013259.

Basu, S., et al. (2001b), Ionospheric effects of major magnetic storms during the International Space Weather Period of September and October 1999: GPS observations, VHF/UHF scintillations, and in situ density structures at middle and equatorial latitudes, *J. Geophys. Res.*, *106*, 30,389–30,413, doi:10.1029/2001JA001116.

Basu, S., Su. Basu, K. M. Groves, E. MacKenzie, M. J. Keskinen, and F. J. Rich (2005), Near-simultaneous plasma structuring in the midlatitude and equatorial ionosphere during magnetic superstorms, *Geophys. Res. Lett.*, *32*, L12S05, doi:10.1029/2004GL021678.

Blanc, M., and A. D. Richmond (1980), The ionospheric disturbance dynamo, *J. Geophys. Res.*, *85*, 1669–1686, doi:10.1029/JA085iA04p01669.

Bowman, G. G. (1982), Spread-F occurrence in mid and low latitude regions related to various levels of geomagnetic activity, *J. Atmos. Sol. Terr. Phys.*, *44*, 585–589.

Burns, A. G., T. L. Killeen, W. Deng, G. R. Carignan, and R. G. Roble (1995), Geomagnetic storm effects in the low- to middle-latitude upper thermosphere, *J. Geophys. Res.*, *100*, 14,673–14,691, doi:10.1029/94JA03232.

Chakrabarty, D., R. Sekar, R. Narayanan, C. V. Devasia, and B. M. Pathan (2005), Evidence for interplanetary electric field effect on the OI 630.0 nm airglow over low latitudes, *J. Geophys. Res.*, *110*, A11301, doi:10.1029/2005JA011221.

Chandra, H., and R. G. Rastogi (1972a), Spread-F at magnetic equatorial station Thumba, *Ann. Geophys.*, *28*, 37–44.

Chandra, H., and R. G. Rastogi (1972b), Solar cycle and seasonal variations of spread-F near magnetic equator, *Ann. Geophys.*, *28*, 709–716.

Chandra, H., and G. D. Vyas (1978), On the relationship between magnetic activity and spread *F* at Kodaikanal, *Indian J. Radio Space Phys.*, *7*, 263–265.

Christensen, A. B., et al. (2003), Initial observations with the Global Ultraviolet Imager (GUVI) in the NASA TIMED satellite mission, *J. Geophys. Res.*, *108*(A12), 1451, doi:10.1029/2003JA009918.

Dabas, R., D. Lakshmi, and B. Reddy (1989), Effect of geomagnetic disturbances on the VHF nighttime scintillation activity at equatorial and low latitudes, *Radio Sci.*, *24*, 563–573, doi:10.1029/RS024i004p00563.

Fejer, B. G. (1986), Equatorial ionospheric electric fields associated with magnetospheric disturbances, in *Solar Wind Magnetosphere Coupling*, edited by Y. Kamide and J. A. Slavin, pp. 519–545, Terra Sci., Tokyo.

Fejer, B. G. (1997), The electrodynamics of the low-latitude ionosphere: Recent results and future challenges, *J. Atmos. Sol. Terr. Phys.*, *59*, 1465–1482, doi:10.1016/S1364-6826(96)00149-6.

Fejer, B. G., and L. Scherliess (1997), Empirical models of storm time equatorial zonal electric fields, *J. Geophys. Res.*, *102*, 24,047–24,056, doi:10.1029/97JA02164.

Fejer, B. G., C. A. Gonzales, D. T. Farley, M. C. Kelley, and R. F. Woodman (1979), Equatorial electric fields during magnetically disturbed conditions: 1. The effect of the interplanetary magnetic field, *J. Geophys. Res.*, *84*, 5797–5802, doi:10.1029/JA084iA10p05797.

Fejer, B. G., M. F. Larsen, and D. T. Farley (1983), Equatorial disturbance dynamo electric fields, *Geophys. Res. Lett.*, *10*, 537–540, doi:10.1029/GL010i007p00537.

Fejer, B. G., R. W. Spiro, R. A. Wolf, and J. C. Foster (1990), Latitudinal variation of perturbation electric fields during magnetically disturbed periods: 1986 SUNDIAL observations and model results, *Ann. Geophys.*, *8*, 441–454.

Fejer, B. G., L. Scherliess, and E. R. de Paula (1999), Effects of the vertical plasma drift velocity on the generation and evolution of equatorial spread *F*, *J. Geophys. Res.*, *104*, 19,859–19,869, doi:10.1029/1999JA900271.

Fejer, B. G., J. T. Emmert, and D. P. Sipler (2002), Climatology and storm time dependence of nighttime thermospheric neutral winds over Millstone Hill, *J. Geophys. Res.*, *107*(A5), 1052, doi:10.1029/2001JA000300.

Field, P. R., H. Rishbeth, R. J. Moffett, D. W. Idenden, T. J. Fuller-Rowell, G. H. Millward, and A. D. Aylward (1998), Modelling composition changes in F-layer storms, *J. Atmos. Sol. Terr. Phys.*, *60*, 523–543, doi:10.1016/S1364-6826(97)00074-6.

Fuller-Rowell, T. J., G. H. Millward, A. D. Richmond, and M. V. Codrescu (2002), Storm-time changes in the upper atmosphere at low latitudes, *J. Atmos. Sol. Terr. Phys.*, *64*, 1383–1391, doi:10.1016/S1364-6826(02)00101-3.

Gonzales, C. A., M. C. Kelley, B. G. Fejer, J. F. Vickrey, and R. F. Woodman (1979), Equatorial electric fields during magnetically disturbed conditions: 2. Implications of simultaneous auroral and equatorial measurements, *J. Geophys. Res.*, *84*, 5803–5812, doi:10.1029/JA084iA10p05803.

Hines, C. O. (1960), Internal atmospheric gravity waves at ionospheric heights, *Can. J. Phys.*, *38*, 1441–1481.

Hines, C. O. (1974), *The Upper Atmosphere in Motion: A Selection of Papers With Annotation*, *Geophys. Monogr.*, vol. 18, 1027 pp., AGU, Washington, D. C.

Huang, C. M., and M. Q. Chen (2008), Formation of maximum electric potential at the geomagnetic equator by the disturbance dynamo, *J. Geophys. Res.*, *113*, A03301, doi:10.1029/2007JA012843.

Huang, C.-M., A. D. Richmond, and M.-Q. Chen (2005), Theoretical effects of geomagnetic activity on low-latitude ionospheric electric fields, *J. Geophys. Res.*, *110*, A05312, doi:10.1029/2004JA010994.

Hysell, D. L., and J. D. Burcham (1998), JULIA radar studies of equatorial spread *F*, *J. Geophys. Res.*, *103*, 29,155–29,167, doi:10.1029/98JA02655.

Jaggi, R. K., and R. A. Wolf (1973), Self-consistent calculation of the motion of a sheet of ions in the magnetosphere, *J. Geophys. Res.*, *78*, 2852–2866, doi:10.1029/JA078i016p02852.

Jing, N., and R. D. Hunsucker (1993), A theoretical investigation of sources of large and medium scale atmospheric gravity waves in the auroral oval, *J. Atmos. Terr. Phys.*, *55*, 1667–1679, doi:10.1016/0021-9169(93)90171-T.

Kelley, M. C., and T. Maruyama (1992), A diagnostic model of equatorial spread *F*, 2, The effect of magnetic activity, *J. Geophys. Res.*, *97*, 1271–1277, doi:10.1029/91JA02607.

Kelley, M. C., B. G. Fejer, and C. A. Gonzales (1979), An explanation for anomalous ionospheric electric fields associated with a northward turning of the interplanetary magnetic field, *Geophys. Res. Lett.*, *6*, 301–304, doi:10.1029/GL006i004p00301.

Kelley, M. C., J. J. Makela, J. L. Chau, and M. J. Nicholls (2003), Penetration of the solar wind electric field into the magnetosphere/ionosphere system, *Geophys. Res. Lett.*, *30*(4), 1158, doi:10.1029/2002GL016321.

Khan, H., and S. W. H. Cowley (1999), Observations of the response time of high latitude ionospheric convection to variations in the interplanetary magnetic field using EISCAT and IMP-8 data, *Ann. Geophys.*, *17*, 1306–1335, doi:10.1007/s00585-999-1306-8.

Kikuchi, T., M. Pinnock, A. Rodger, H. Luehr, T. Kitamura, H. Tachihara, M. Watanabe, N. Sato, and M. Ruohoniemi (2000a), Global evolution of a substorm-associated DP2 current system observed by SuperDARN and magnetometers, *Adv. Space Res.*, *26*, 121–124, doi:10.1016/S0273-1177(99)01037-6.

Kikuchi, T., H. Luehr, K. Schlegel, H. Tachihara, M. Shinohara, and T.-I. Kitamura (2000b), Penetration of auroral electric fields to the equator during a substorm, *J. Geophys. Res.*, *105*, 23,251–23,261, doi:10.1029/2000JA900016.

Kikuchi, T., K. K. Hashimoto, T.-I. Kitamura, H. Tachihara, and B. Fejer (2003), Equatorial counterelectrojets during substorms, *J. Geophys. Res.*, *108*(A11), 1406, doi:10.1029/2003JA009915.

Kikuchi, T., K. H. Hashimoto, and K. Nazoki (2008), Penetration of magnetospheric electric fields to the equator during a geomagnetic storm, *J. Geophys. Res.*, *113*, A06214, doi:10.1029/2007JA012628.

Kobea, A. T., C. Amory-Mazaudier, J. M. Do, H. Luehr, E. Hougninou, J. Vassal, E. Blanc, and J. J. Curto (1998), Equatorial electrojet as part of the global circuit: A case-study from the IEEY, *Ann. Geophys.*, *16*, 698–710, doi:10.1007/s00585-998-0698-1.

Kobea, A. T., A. D. Richmond, B. A. Emery, C. Peymirat, H. Luehr, T. Moretto, M. Hairston, and C. Amory-Mazaudier (2000), Electrodynamic coupling of high and low latitudes: Observations on May 27, 1993, *J. Geophys. Res.*, *105*, 22,979–22,989, doi:10.1029/2000JA000058.

Lin, C. H., A. D. Richmond, J. Y. Liu, H. C. Yeh, L. J. Paxton, G. Lu, H. F. Tsai, and S.-Y. Su (2005), Large-scale variations of the low-latitude ionosphere during the October-November 2003 superstorm: Observational results, *J. Geophys. Res.*, *110*, A09S28, doi:10.1029/2004JA010900.

Liu, C. H., and B. Edwards (1988), *WITS Handbook, World Ionosphere/Thermosphere Study*, vol. 2, Natl. Sci. Found., Urbana, Ill.

Lyon, A., N. Skinner, and R. Wright (1960), The belt of equatorial spread-F, *J. Atmos. Terr. Phys.*, *19*, 145–159, doi:10.1016/0021-9169(60)90043-X.

Mannucci, A. J., B. T. Tsurutani, B. A. Iijima, A. Komjathy, A. Saito, W. D. Gonzalez, F. L. Guarnieri, J. U. Kozyra, and R. Skoug (2005), Dayside global ionospheric response to the major interplanetary events of October 29–30, 2003 "Halloween Storms," *Geophys. Res. Lett.*, *32*, L12S02, doi:10.1029/2004GL021467.

Maruyama, T., G. Ma, and M. Nakamura (2004), Signature of TEC storm on 6 November 2001 derived from dense GPS receiver network and ionosonde chain over Japan, *J. Geophys. Res.*, *109*, A10302, doi:10.1029/2004JA010451.

Mazaudier, C., and S. V. Venkateswaran (1990), Delayed ionospheric effects of the geomagnetic storms of March 22, 1979, studied by the sixth coordinated data analysis workshop (CDAW-6), *Ann. Geophys.*, *8*, 511–518.

Meier, R. R., G. Crowley, D. J. Strickland, A. B. Christensen, L. J. Paxton, D. Morrison, and C. L. Hackeert (2005), First look at the 20 November superstorm with TIMED/GUVI: Comparisons with a thermospheric global circulation model, *J. Geophys. Res.*, *110*, A09S41, doi:10.1029/2004JA010990.

Nishida, A. (1968), Coherence of geomagnetic *DP* 2 fluctuations with interplanetary magnetic variations, *J. Geophys. Res.*, *73*, 5549–5559, doi:10.1029/JA073i017p05549.

Ossakow, S. L. (1981), Spread *F* theories: A review, *J. Atmos. Terr. Phys.*, *43*, 437–452.

Pandey, R., and N. Dashora (2006), Space weather studies at the crest of the equatorial ionization anomaly using GPS receiver, paper presented at XXVIIIth General Assembly of URSI, New Delhi, India, 23–29 Oct. 2005.

Paxton, L. J., et al. (1999), Global ultraviolet imager (GUVI): Measuring composition and energy inputs for the NASA Thermosphere Ionosphere Mesosphere Energetics and Dynamics (TIMED) mission, *Proc. SPIE Int. Soc. Opt. Eng.*, *3756*, 265–276.

Paxton, L. J., et al. (2004), GUVI: A hyperspectral imager for geospace, *Proc. SPIE Int. Soc. Opt. Eng.*, *5660*, 227–240, doi:10.1117/12/579171.

Prolss, G. W. (1997), Magnetic storm perturbations of the upper atmosphere, in *Magnetic Storms*, *Geophys. Monogr. Ser.*, vol. 98, edited by B. T. Tsurutani et al., pp. 227–241, AGU, Washington, D. C.

Rastogi, R. G. (1977), Geomagnetic storms and electric fields in the equatorial ionosphere, *Nature*, *268*, 422–424, doi:10.1038/268422a0.

Rastogi, R. G. (1997), Midday reversal of equatorial ionospheric electric field, *Ann. Geophys.*, *15*, 1309–1315, doi:10.1007/s00585-997-1309-2.

Rastogi, R. G., and J. A. Klobuchar (1990), Ionospheric electron content within the equatorial F_2 layer anomaly belts, *J. Geophys. Res.*, *95*, 19,045–19,052, doi:10.1029/JA095iA11p19045.

Rastogi, R. G., and V. L. Patel (1975), Effect of interplanetary magnetic field on the ionosphere over the magnetic equator, *Proc. Indian Acad. Sci.*, *82*, 121–141.

Rastogi, R. G., and R. F. Woodman (1978), Spread-F in equatorial ionograms associated with reversal of horizontal F region electric field, *Ann. Geophys.*, *34*, 31–36.

Rastogi, R. G., G. D. Vyas, and H. Chandra (1978), Geomagnetic disturbance effects on equatorial spread-F at Huancayo, *Proc. Indiana Acad. Sci.*, *87A*, 109–113.

Rastogi, R. G., J. Mullen, and E. MacKenzie (1981), Effect of geomagnetic activity on equatorial radio VHF scinitllation and spread *F*, *J. Geophys. Res.*, *86*, 3661–3664, doi:10.1029/JA086iA05p03661.

Reddy, C. A., V. V. Somayajulu, and C. V. Devisia (1978), Global scale electrodynamical coupling of the auroral and equatorial dynamo regions, *J. Atmos. Terr. Phys.*, *41*, 189–201.

Richmond, A. D. (1978), Gravity wave generation, propagation, and dissipation in the thermosphere, *J. Geophys. Res.*, *83*, 4131–4145, doi:10.1029/JA083iA09p04131.

Sastri, J. H. (1988), Equatorial electric fields of ionospheric disturbance dynamo origin, *Ann. Geophys.*, *6*, 635–642.

Sastri, J. H., J. V. S. V. Rao, and K. B. Ramesh (1993), Penetration of polar electric field to the nightside dip equator at times of geomagnetic sudden commencements, *J. Geophys. Res.*, *98*, 17,517–17,523, doi:10.1029/93JA00418.

Sastri, J. H., M. A. Abdu, and J. H. A. Sobral (1997), Response of equatorial ionosphere to episodes of asymmetric ring current activity, *Ann. Geophys.*, *15*, 1316–1323, doi:10.1007/s00585-997-1316-3.

Sastri, J. H., N. Jyoti, V. V. Somayajulu, H. Chandra, and C. V. Devasia (2000), Ionospheric storm of early November 1993 in the Indian equatorial region, *J. Geophys. Res.*, *105*, 18,443–18,455, doi:10.1029/1999JA000372.

Senior, C., and M. Blanc (1984), On the control of magnetospheric convection by the spatial distribution of ionospheric conductivities, *J. Geophys. Res.*, *89*, 261–284, doi:10.1029/JA089iA01p00261.

Sobral, J. H. A., M. A. Abdu, W. D. Gonzalez, B. T. Tsurutani, I. S. Batista, and A. C. de Gonzalez (1997), Effects of intense storms and substorms on the equatorial ionosphere/thermosphere system in the American sector from ground based and satellite data, *J. Geophys. Res.*, *102*, 14,305–14,313, doi:10.1029/97JA00576.

Sobral, J. H. A., M. A. Abdu, C. S. Yamashita, W. D. Gonzalez, A. C. de Gonzalez, I. S. Batista, C. J. Zamlutti, and B. T. Tsurutani (2001), Responses of the low-latitude ionosphere to very intense geomagnetic storms, *J. Atmos. Sol. Terr. Phys.*, *63*, 965–974, doi:10.1016/S1364-6826(00)00197-8.

Somayajulu, V. V., C. A. Reddy, and K. S. Viswanathan (1987), Penetration of magnetospheric convective electric field to the equatorial ionosphere during the substorm of March 22, 1979, *Geophys. Res. Lett.*, *14*, 876–879, doi:10.1029/GL014i008p00876.

Southwood, D. J. (1977), The role of hot plasma in magnetospheric convection, *J. Geophys. Res.*, *82*, 5512–5520, doi:10.1029/JA082i035p05512.

Spiro, R. W., R. A. Wolf, and B. G. Fejer (1988), Penetration of high latitude electric field effects to low latitude during SUNDIAL, 1984, *Ann. Geophys.*, *6*, 39–50.

Sultan, P. (1996), Linear theory and modeling of the Rayleigh-Taylor instability leading to the occurrence of equatorial spread *F*, *J. Geophys. Res.*, *101*, 26,875–26,891, doi:10.1029/96JA00682.

Tsurutani, B. T., et al. (2004), Global dayside ionospheric uplift and enhancement associated with interplanetary electric field, *J. Geophys. Res.*, *109*, A08302, doi:10.1029/2003JA010342.

Tulasi Ram, S., P. V. S. Rama Rao, D. S. V. V. D. Prasad, K. Niranjan, S. Gopi Krishna, R. Sridharan, and S. Ravindran (2008), Local time dependent response of postsunset ESF during geomagnetic storms, *J. Geophys. Res.*, *113*, A07310, doi:10.1029/2007JA012922.

Vasyliunas, V. M. (1972), The interrelationship of magnetospheric processes, in *Earth's Magnetospheric Processes*, edited by B. M. McCormac, pp. 29–38, D. Reidel, Norwell, Mass.

Zhao, B., W. Wan, and L. Liu (2005), Response of equatorial anomaly to the October-November 2003 superstorm, *Ann. Geophys.*, *23*, 693–706, doi:10.5194/angeo-23-693-2005.

M. S. Bagiya, K. N. Iyer, and H. P. Joshi, Department of Physics, Saurashtra University, Rajkot 360005, India. (bagiyamala@gmail.com)

B. M. Pathan, Indian Institute of Geomagnetism, Navi Mumbai 410218, India.

S. Ravindran and R. Sridharan, Space Physics Laboratory, Vikram Sarabhai Space Centre, Trivandrum 695022, India.

S. V. Thampi, Research Institute for Sustainable Humanosphere, Kyoto University, Kyoto 611-0011, Japan.

T. Tsugawa, National Institute of Information and Communications Technology, 4-2-1 Nukui-Kitamachi, Koganei, Tokyo 184-8795, Japan.